Stanford Exploration Project, Report 108, April 29, 2001, pages 1–??

Imaging under salt edges: A regularized least-squares inversion scheme

Marie L. Prucha, Robert G. Clapp, and Biondo L. Biondi[1]

ABSTRACT

We introduce a method for improving the image in areas of poor illumination using least-squares inversion regularized with dip penalty filters in one and two dimensions. The use of these filters helps to emphasize the weak energy that exists in poorly illuminated areas, and fills-in gaps by assuming lateral continuity along the reflection-angle axis and/or the midpoint axes. We tested our regularized inversion method on synthetic and real data. The inversion employing one-dimensional filters along the reflection-angle axis generated prestack images significantly better than the images obtained by simple migration and unregularized inversion. The inversion employing two-dimensional filters reduced the frequency of the image but also increased reflectors' continuity and reduced noise.

INTRODUCTION

Seismic energy that propagates through a complex subsurface can easily be directed outside of the bounds of our survey, causing poor illumination. Additionally, energy that does stay inside the bounds of our survey will be attenuated as some of it becomes evanescent. It is impossible to create a survey of infinite length and we have little control over the formation of evanescent waves, so we have to try to make due with the data we can collect. This data will have areas of poor illumination where noise makes it impossible for us to find the real event. Therefore, we need to try to remove noise and make the event more visible.

Illumination problems generally occur in areas where the subsurface is complex. This means that there are also likely to be artifacts caused by multipathing. To get around this, we choose to work in the angle domain, which doesn't allow multipathing (Xu et al., 1998). The methodology we follow to carry out processing in the angle domain has been explained by Prucha et al. (1999).

Reducing multipathing artifacts is not enough to overcome poor illumination. We are trying to improve our model by using a preconditioned inversion scheme. This scheme uses dip penalty filters (Clapp et al., 1997) which can be applied in the common midpoint (CMP) - depth plane, the reflection angle - depth plane (Prucha et al., 2000), or both.

This paper will explain the theory behind our inversion method and the use of our dip

[1]**email:** marie@sep.stanford.edu,bob@sep.stanford.edu,biondo@sep.stanford.edu

penalty filters. Then we will show the results of using this method on a synthetic dataset and on some real 2-D data. Finally, we will discuss the problems we still must solve and our plans for the future.

THEORY

One of the most common processing steps taken with data from complex areas is migration. Unfortunately, it is also well-known that migration does not provide the best possible model (Duquet and Marfurt, 1999; Ronen and Liner, 2000). It is possible to get a better model by inversion. However, inversion alone is not enough to fill in areas of poor illumination. Fortunately, we often have some idea of how we think events *should* behave in areas of poor illumination, so we can impose our idea through a regularization operator. This can be represented by these familiar equations:

$$\begin{aligned} \mathbf{d} &\approx \mathbf{L}\mathbf{m} \\ 0 &\approx \epsilon \mathbf{A}\mathbf{m} \end{aligned} \tag{1}$$

where $\mathbf{d}$ and $\mathbf{m}$ are the data and model, respectively, $\mathbf{L}$ is the angle domain modeling operator described by Prucha et al. (1999), and $\mathbf{A}$ is the regularization operator. A simple substitution of variables can help reduce the number of iterations necessary (Fomel et al., 1997). This substitution is $\mathbf{m} = \mathbf{A^{-1}p}$ where $\mathbf{m}$ is the model and $\mathbf{p}$ is our new variable. This gives us a new set of equations:

$$\begin{aligned} \mathbf{d} &\approx \mathbf{L}\mathbf{A^{-1}}\mathbf{p} \\ 0 &\approx \epsilon \mathbf{p}. \end{aligned} \tag{2}$$

The inverse operator $\mathbf{A^{-1}}$ is applied using helical polynomial division (Claerbout, 1998). We chose to make the operator $\mathbf{A^{-1}}$ a smoothing operator that would act along a specified dip. This operator was constructed from dip penalty, or steering, filters (Clapp et al., 1997). We implemented these filters in 2-D by cascading them (Clapp, 2000). This cascaded method means that our preconditioning operator $\mathbf{A^{-1}}$ is a combination of two preconditioning operators in different dimensions:

$$\mathbf{A^{-1}} \;=\; \mathbf{A_{\alpha z}^{-1}}\mathbf{A_{xz}^{-1}} \tag{3}$$

where $\mathbf{A_{xz}^{-1}}$ are filters that are constructed from dips along reflectors in the CMP-depth plane. These filters smooth along chosen reflectors (Figures 4 and 12). The second term, $\mathbf{A_{\alpha z}^{-1}}$, are filters in the angle-depth plane and, because we assume we are using the correct velocity, we simply smooth horizontally.

One potential drawback to this cascading method is that it can introduce anisotropy to the events, depending on the strength and direction of the dip penalty filters in each dimension. Fomel (2000) describes a method using spectral factorization that may eliminate this anisotropy, but at this early stage we have not determined if such a solution is necessary.

By imposing these smoothing conditions on the model and doing iterative inversion, we hope to fill in areas that do contain real information while smoothing and removing the noise.

RESULTS

Synthetic data

We applied our methodology to a synthetic 2-D dataset. This dataset was provided to us by SMART JV and is designed to have serious illumination problems. A common angle section from the migration of this dataset can be seen in Figure 1. We are particularly interested in the area beneath the edge of the salt. As you can see inside the oval drawn on Figure 1, the amplitude of the reflectors decreases very sharply underneath the salt. Also, there is a lot of noise under the salt edge. This is not a surprise since this is a prestack section.

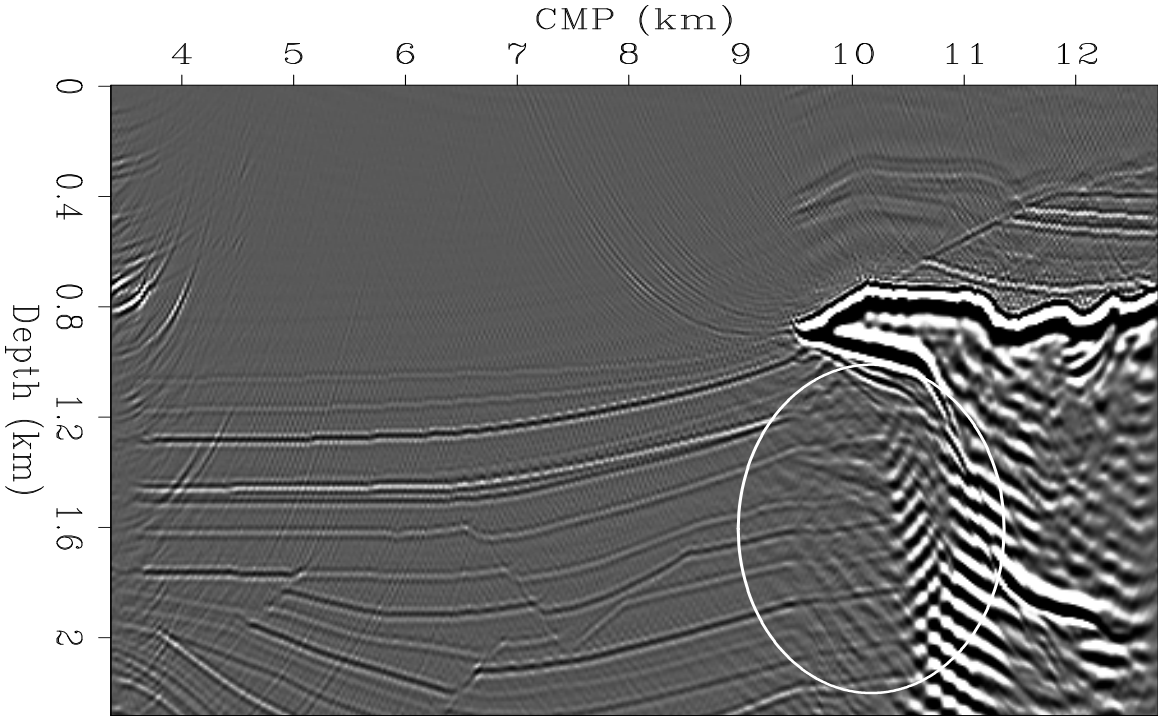

Figure 1: Constant angle panel from migration. marie1-syn.mig [CR]

We first applied just an inversion to this data, with no type of regularization. Inversion is simply the first equation from the set shown in equation (1). Figure 2 shows a constant angle panel after 8 iterations. This result looks even worse than the migration result.

We then applied regularization only in the angle - depth direction. Figure 3 shows a constant angle section after 5 iterations of the method described above. Within the oval we can see that the amplitude along the reflectors is more constant. The reflectors can almost be traced all of the way to the salt. The noise under the salt is much weaker than is seen in the migrated result. The image of the salt flank is also sharper than in the migration result.

Finally, we applied regularization in both directions described in the theory section. To do so, we first picked reflectors from the stacked migration (Figure 4). As you can see, we

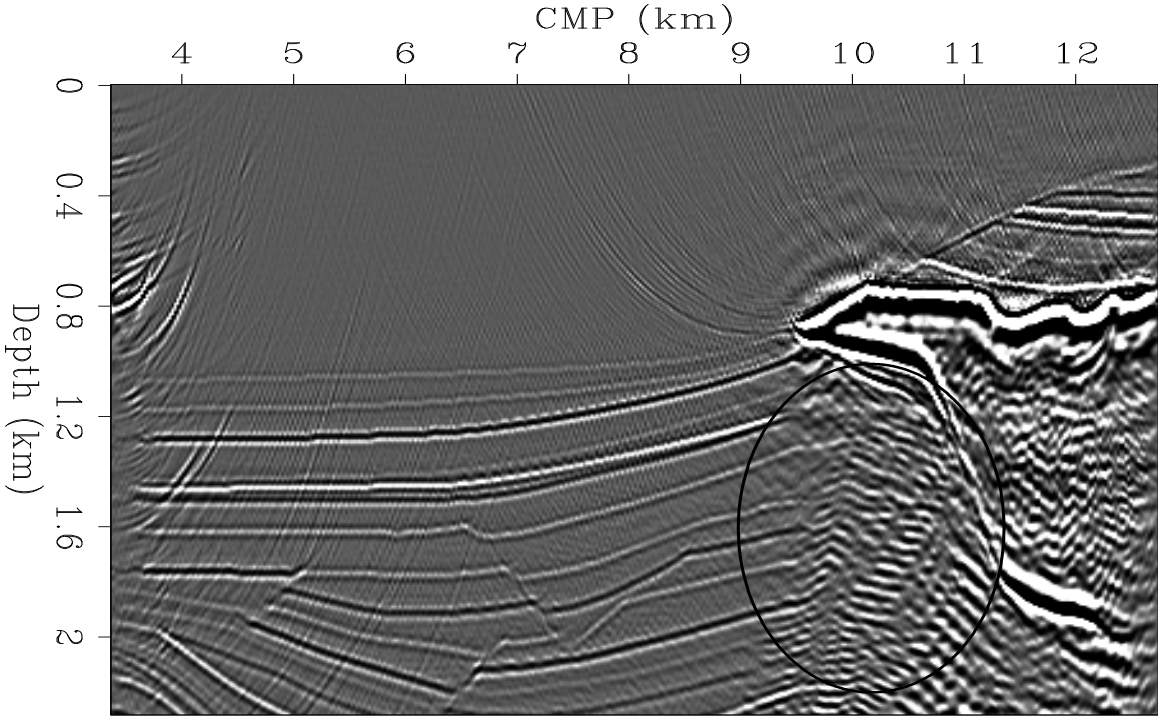

Figure 2: Constant angle panel using inversion only. marie1-syn.inver [CR]

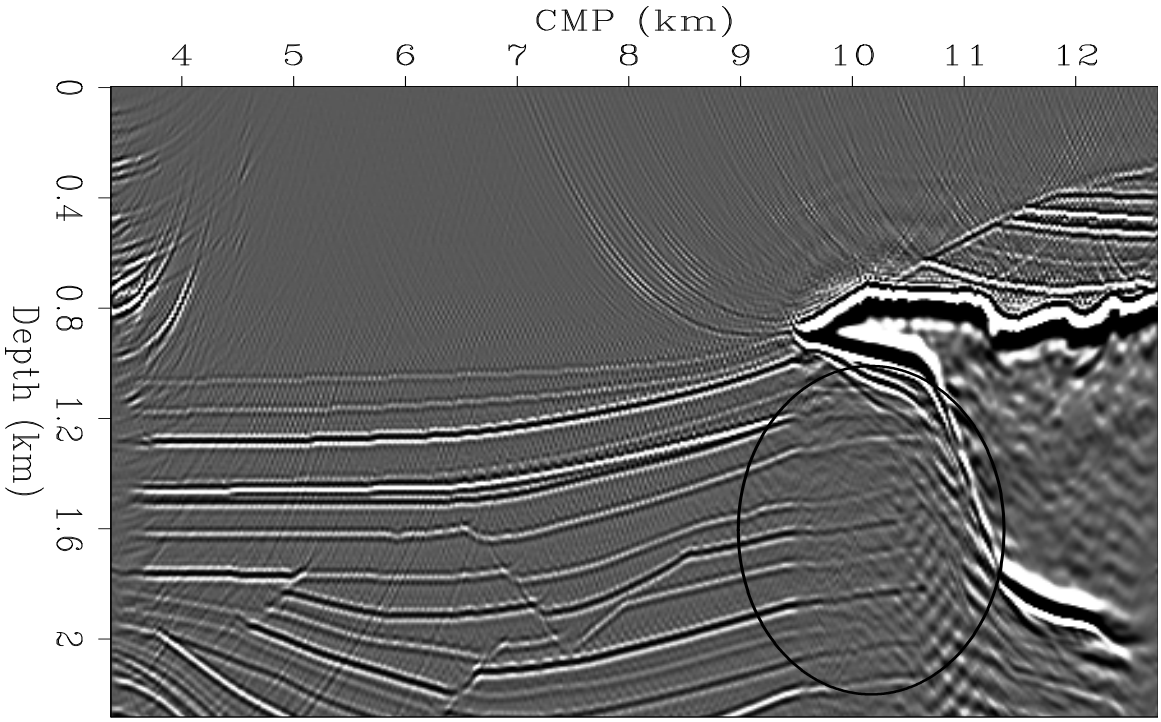

Figure 3: Constant angle panel with preconditioning only along the angle axis. marie1-syn.1dprec [CR]

extended our picked reflectors beyond what can be seen in the migration (Figure 1), in the way that seems most reasonable.

Figures 5 and Figure 6 show the constant angle panel after one and five iterations. The reflectors continue at almost a constant amplitude as far as they were picked in Figure 4, then even farther with decreasing amplitude. More iterations increase the amplitudes. Unfortunately, increasing the number of iterations also decreases the frequency of the data. Even the first iteration causes a slight decrease in frequency. Although these sections look artificial because of the smoothing, we have also cleaned up almost all of the noise. These results seem promising.

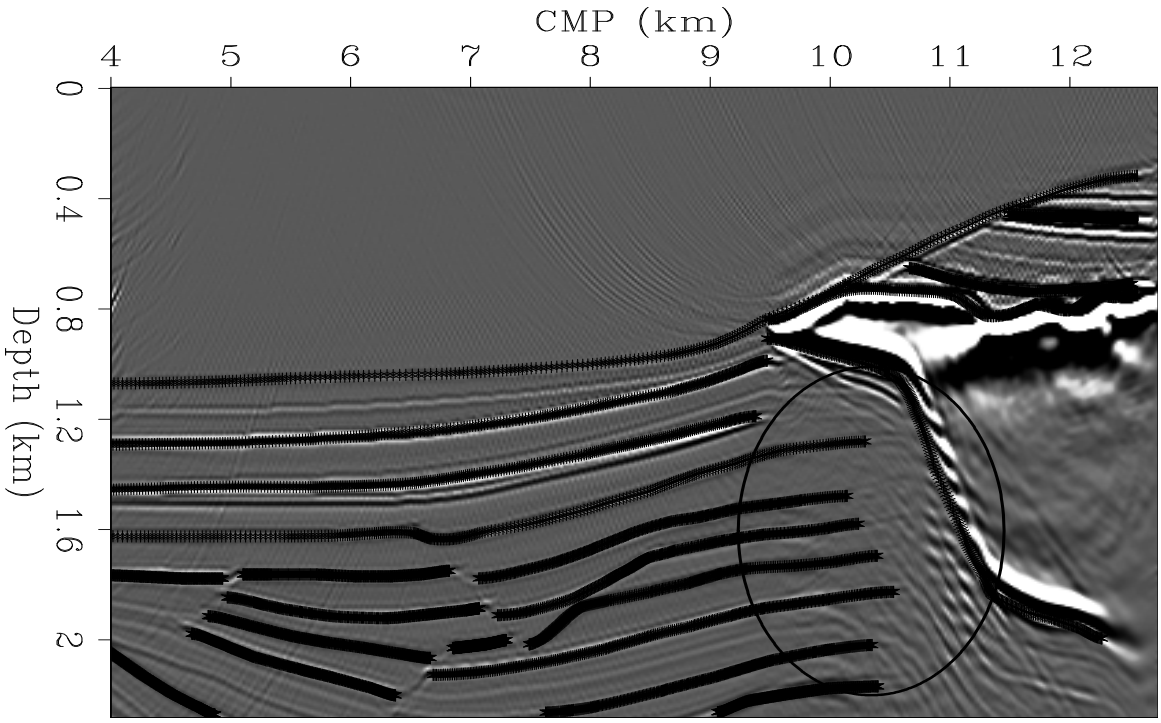

Figure 4: Stacked migration with picked reflectors overlaid. The dip penalty filters smooth along these reflectors. marie1-syn.over [CR]

We can also analyze the effects of inversion and regularization in Angle-Domain Common Image Gathers (ADCIG). Figure 7 shows an ADCIG from the migrated image. Figure 8 shows the same gather after inversion with no regularization. It is actually noisier than the migration result, although the real reflectors are also stronger. Figure 9 is the same ADCIG with regularization only along the angle axis. This gather is smoother and less noisy than the migrated angle gather and the inverted gather. The real reflectors are easier to see. For example, the reflection at depth of about 1.6 km can be followed all the way across the angle axis. In the ADCIG obtained by migration (Figure 7) the same reflection is visible only at small offset ray parameters. Figure 10 shows the same angle gather after five iterations of 2-D preconditioning. This gather is much smoother, with more constant amplitudes, and almost all of the noise is gone. It is possible to see where the preconditioning tries to fill in for the

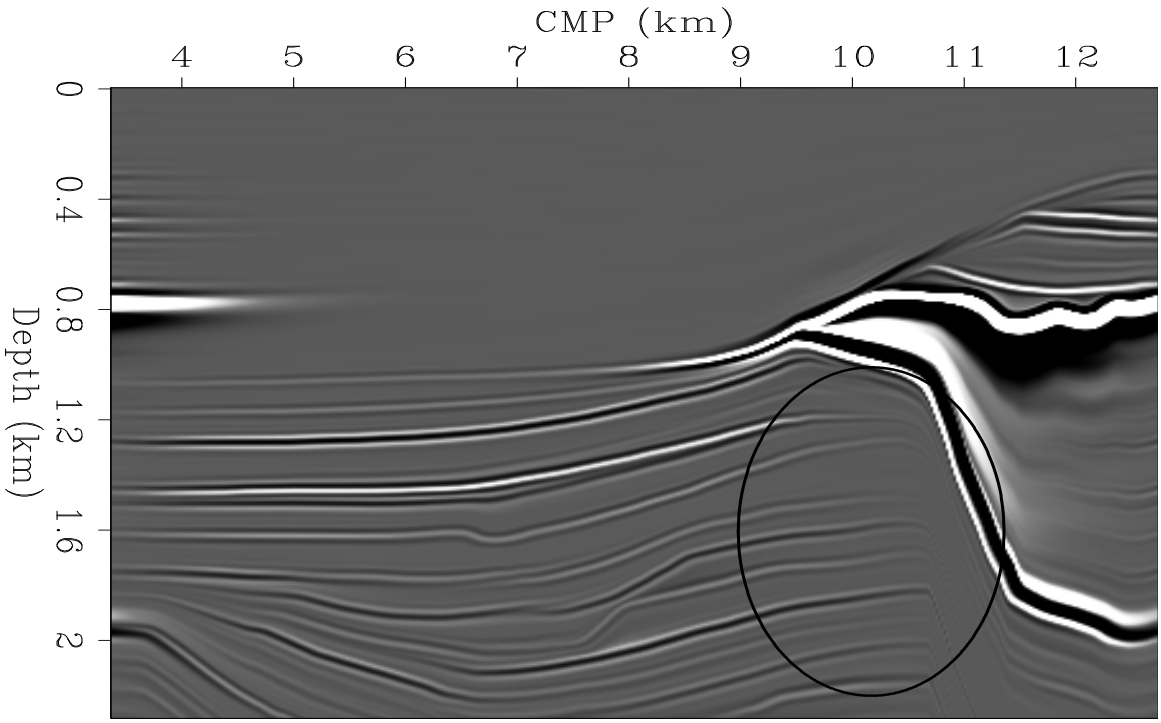

Figure 5: Constant angle panel with one iteration of 2-D preconditioning. marie1-syn.prec.1iter [CR]

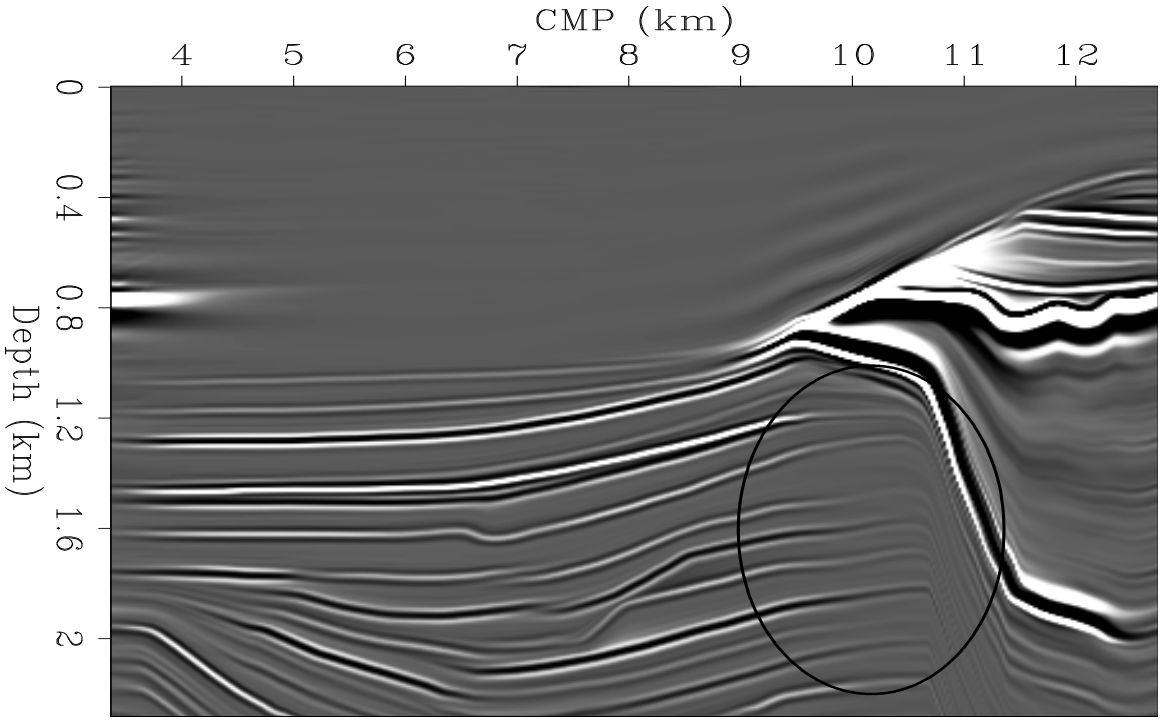

Figure 6: Constant angle panel with five iterations of 2-D preconditioning. marie1-syn.prec.5iter [CR]

reflectors that can't normally be imaged due to our limited survey geometry. It does seem that the preconditioning may be too strong, but the results are encouraging.

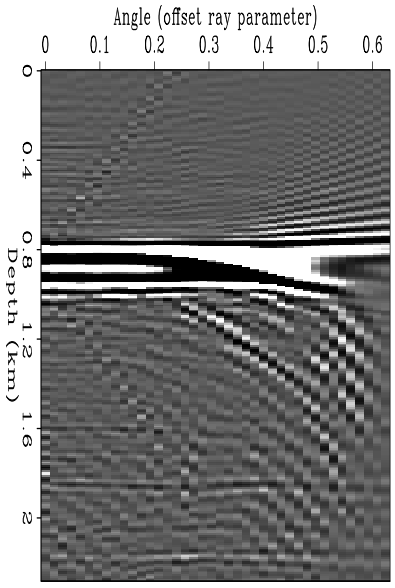

Figure 7: Migrated angle gather from CMP location 9.9 km. marie1-syn.mig.ang [CR]

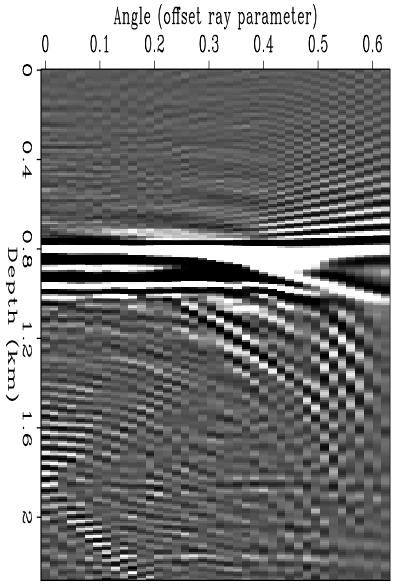

Figure 8: Inverted angle gather from CMP location 9.9 km. marie1-syn.inver.ang [CR]

Real data

We applied our preconditioning method to a 2-D line from the 3-D Elf North Sea dataset. The results are encouraging. Figure 11 is the migrated stack of the 2-D line. Figure 13 is the result of 1 iteration of the preconditioned inversion. Note the the inversion result is lower frequency than the migration. Also, by comparing the inversion result with the picked reflectors (Figure 12) we can see that the smoothing is too strong and may smooth poorly where there are no reflectors picked. Overall, the result looks too artificial.

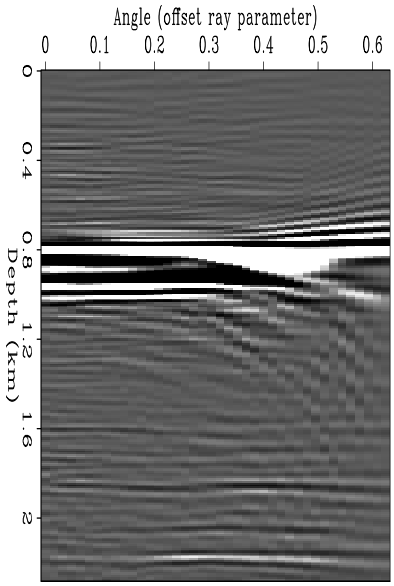

Figure 9: Angle gather after 5 iterations of preconditioning only along the angle axis at CMP location 9.9 km. marie1-syn.1dprec.ang [CR]

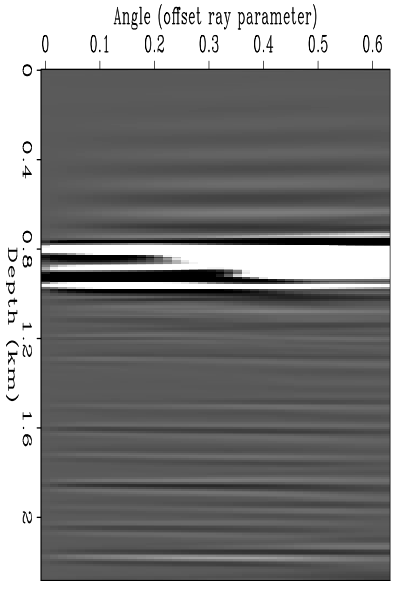

Figure 10: Angle gather after 5 iterations of 2-D preconditioning at CMP location 9.9 km. marie1-syn.prec.ang [CR]

Performing more iterations helps to increase the frequency content of the inversion result. Figure 14 shows the result of five iterations. Although it is higher frequency than Figure 13, it still looks artificial.

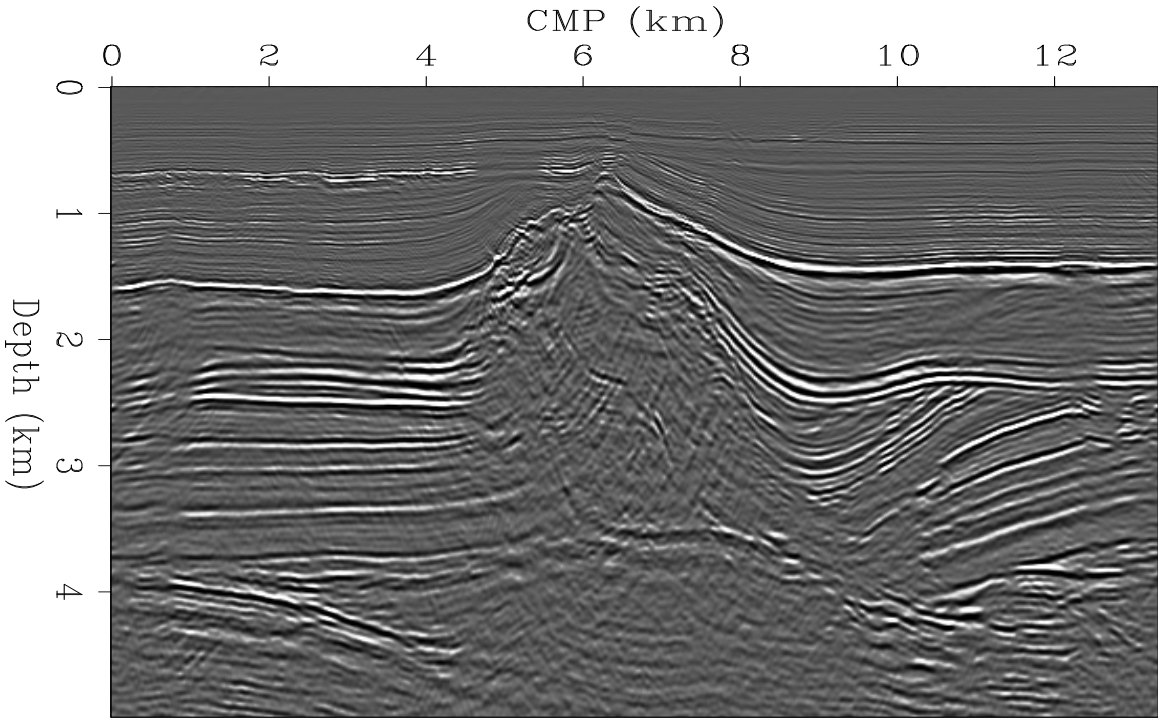

Figure 11: Stacked migration marie1-mig.stack [CR]

We can also consider the results of the smoothing along the angle axis. Figure 15 shows the angle gather that results from migration. Figure 16 is the angle gather after 3 iterations of preconditioned inversion. The preconditioned result is lower frequency and smoothes energy all across the gather, but it is possible to see where the true events end on the preconditioned results. This shows where the linear operator **L** from equations (1) and (2) stops operating and where the preconditioner $\mathbf{A^{-1}}$ takes over. The events change in character as they are smoothed across angles where our survey geometry does not provide large angle information.

CONCLUSIONS AND PLANS

The inversion results obtained by regularizing the inversion process with one-dimensional filters are significantly better than the results of simple migration. We plan to apply soon this method to the real data set shown in this paper. The inversion results obtained by regularizing the inversion process with two-dimensional filters are lower frequency and more artificial looking than we want them to be. We have found that we can increase the frequency content by increasing the rate of depth sampling. However, doubling the sample rate increases the computational cost. We would prefer to find a solution that can solve both the frequency and the appearance problems.

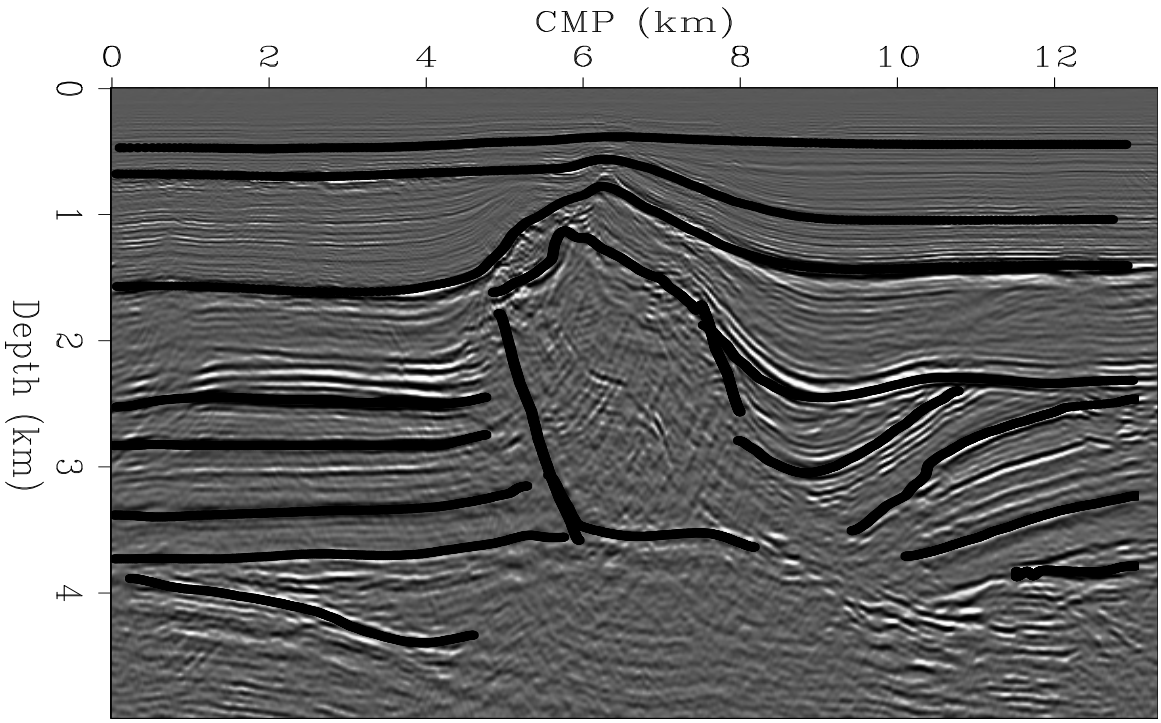

Figure 12: Stacked migration with picked reflectors. Dip penalty filters smooth along a dip field created from the picked reflectors. marie1-overlay [CR]

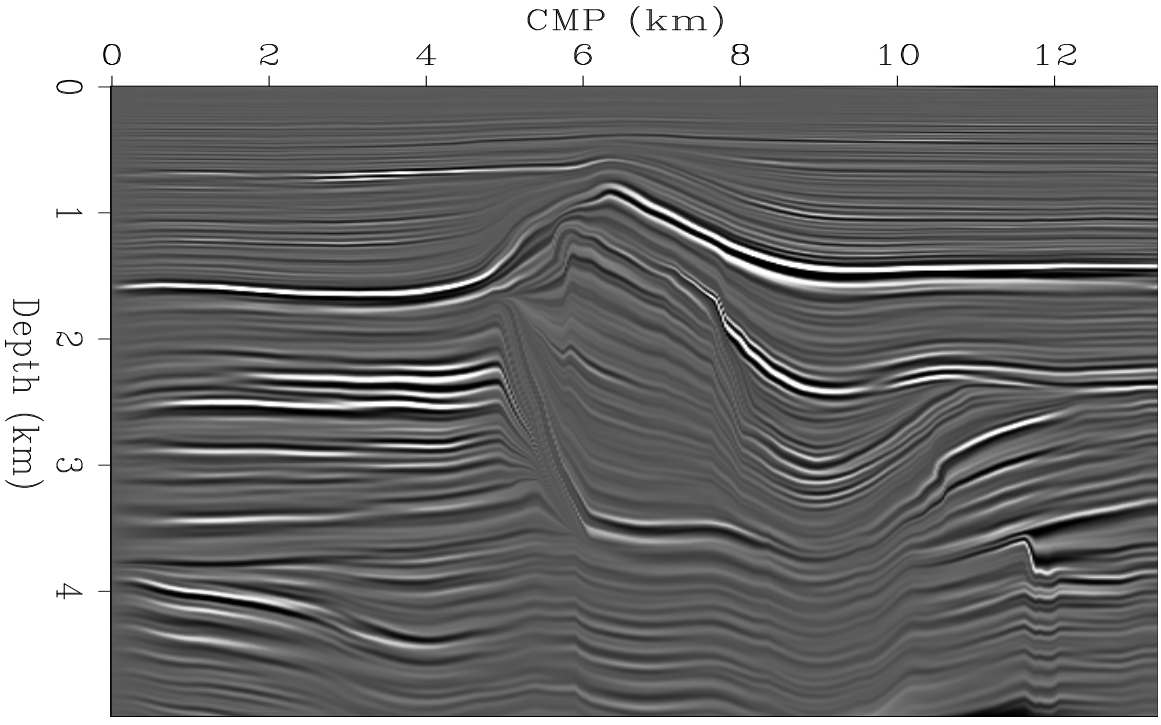

Figure 13: Zero angle panel after one iteration of preconditioned inversion. Note the helix wrap arround artifact at 0.8 km. marie1-prec.1iter [CR]

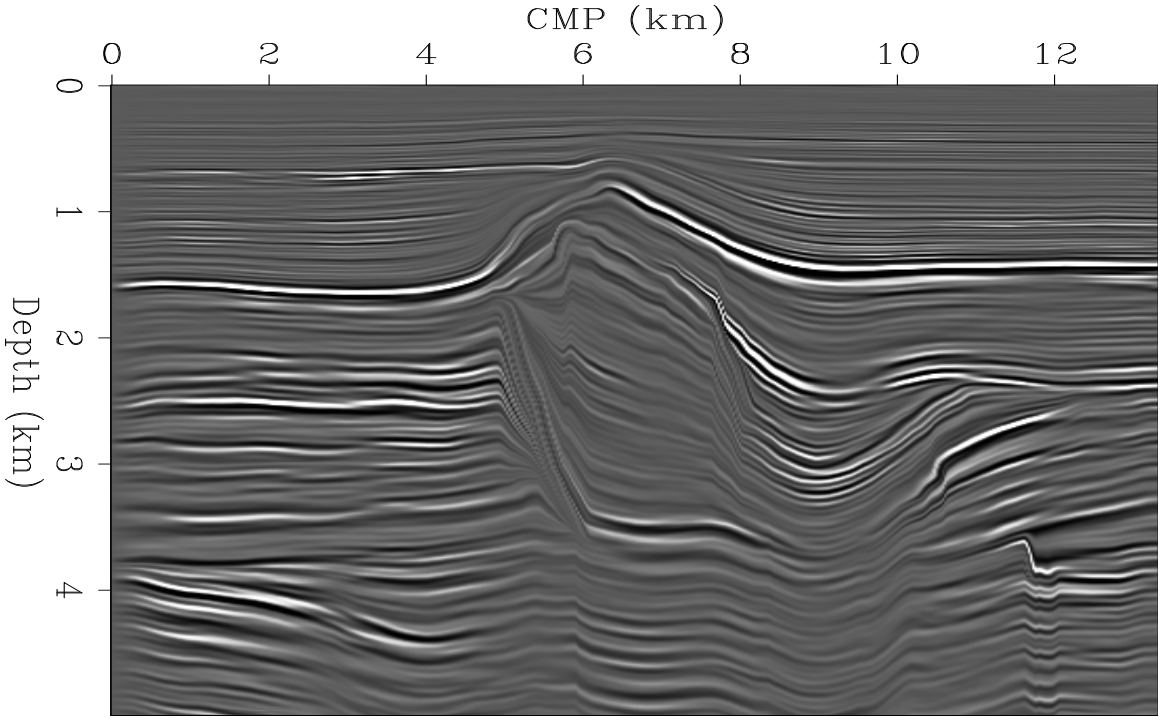

Figure 14: Zero angle panel after five; iterations of preconditioned inversion. marie1-prec.5iter [CR]

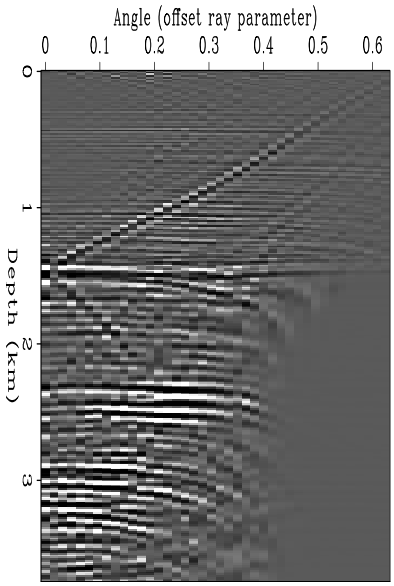

Figure 15: Migrated angle gather marie1-mig.ang [CR]

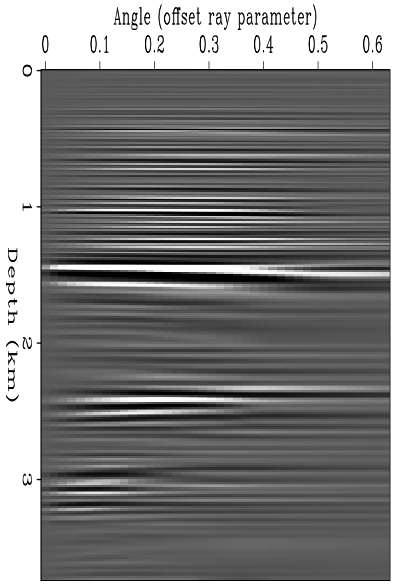

Figure 16: Angle gather after 3 iterations of preconditioned inversion marie1-prec.ang [CR]

We are hoping to use this method to fill in areas of poor illumination. This means that it can be used on a specific target. This can be partially done by downward continuing the data to a depth just above the region of interest, then following the described inversion scheme just over the target area. Additionally, we want to find a way to apply the smoothing on just one reflector or at least in a small area. This would leave the frequency content and appearance of the rest of the image near that of the migrated image.

ACKNOWLEDGMENTS

We would like to thank SMART JV for the synthetic dataset used in this report and TotalFinaElf for the real data.

REFERENCES

Claerbout, J., 1998, Multidimensional recursive filters via a helix: Geophysics, **63**, no. 5, 1532–1541.

Clapp, R. G., Fomel, S., and Claerbout, J., 1997, Solution steering with space-variant filters: SEP–**95**, 27–42.

Clapp, R., 2000, Multiple realizations using standard inversion techniques: SEP–**105**, 67–78.

Duquet, B., and Marfurt, K. J., 1999, Filtering coherent noise during prestack depth migration: Geophysics, **64**, no. 4, 1054–1066.

Fomel, S., Clapp, R., and Claerbout, J., 1997, Missing data interpolation by recursive filter preconditioning: SEP–**95**, 15–25.

Fomel, S., 2000, Applications of plane-wave destructor filters: SEP–**105**, 1–26.

Prucha, M. L., Biondi, B. L., and Symes, W. W., 1999, Angle-domain common image gathers by wave-equation migration: SEP–**100**, 101–112.

Prucha, M. L., Clapp, R. G., and Biondi, B., 2000, Seismic image regularization in the reflection angle domain: SEP–**103**, 109–119.

Ronen, S., and Liner, C. L., 2000, Least-squares DMO and migration: Geophysics, **65**, no. 5, 1364–1371.

Xu, S., Chauris, H., Lambare, G., and Noble, M., 1998, Common angle image gather - A strategy for imaging complex media: 68th Annual Internat. Mtg., Society of Exploration Geophysicists, Expanded Abstracts, 1538–1541.